Cooperation or Coordination of Underwater Glider Networks? An Assessment from Observing System Simulation Experiments in the Ligurian Sea

A. ALVAREZ

Centre for Maritime Research and Experimentation, Science and Technology Organization, NATO, La Spezia, Italy

B. MOURRE

Balearic Islands Coastal Observing and Forecasting System, Palma de Mallorca, Spain

(Manuscript received 10 October 2013, in final form 11 June 2014)

ABSTRACT

The coordinated and cooperative-unaware networking of glider fleets have been proposed to obtain a performance gain in ocean sampling over naïve collective behavior. Whether one of these implementations results in a more efficient sampling of the ocean variability remains an open question. This article aims at a performance evaluation of cooperative-unaware and coordinated networks of gliders to reduce the uncertainty in operational temperature model predictions. The evaluation is based on an observing system simulation experiment (OSSE) implemented in the northern Ligurian Sea (western Mediterranean) from 21 August to 1 September 2010. The OSSE confronts the forecast skills obtained by the Regional Ocean Modeling System (ROMS) when assimilating data gathered from a cooperative and unaware network of three gliders with the prediction skill obtained when data comes from a coordinated configuration. An asynchronous formulation of the ensemble Kalman filter with a 48-h window is used to assimilate simulated temperature observations. Optimum sampling strategies of the glider networks, based on a pattern search optimization algorithm, are computed for each 48-h forecasting period using a covariance integrated in time and in the vertical direction to reduce the dimensionality of the problem and to enable a rapid resolution. Perturbations of the depth-averaged current field in glider motions are neglected. Results indicate a better performance of the coordinated network configuration due to an enhanced capacity to capture an eddy structure that is responsible for the largest forecast error in the experimental domain.

1. Introduction

Autonomous underwater gliders (AUGs) have raised a particular interest among oceanographers for their maneuverability, autonomy, and long endurance at sea (Kunzig 1996; Bachmayer et al. 2004; Rudnick et al. 2004; Testor et al. 2010). Gliders make use of buoyancy changes, hydrodynamic shape, and small fins to induce net horizontal motions while controlling their buoyancy (Eriksen et al. 2001; Sherman et al. 2001; Webb et al. 2001). This propelling procedure implies low energy consumption, facilitating long time periods of operation at sea without the need for human intervention. For this reason, AUGs are becoming essential components of ocean observatories (Dickey 2003).

Cooperation of a fleet of gliders can substantially increase the efficiency, reliability, and robustness of oceanographic sampling missions. Following the networking taxonomy defined by Farinelli et al. (2004) for multirobot systems, a cooperative-unaware glider network is a fleet of gliders with a common global goal to achieve but in which each glider does not have knowledge of the rest of the platforms in the fleet. Instead, a glider network is said to be coordinated when each glider exerts its influence on the behavior of other gliders when pursuing a common goal (e.g., when the fleet is constrained to follow a geometrical formation).

Ocean sampling with networked autonomous sensors was introduced by Curtin et al. (1993) 20 years ago. Since then, significant effort has been done to achieve the operational implementation of Autonomous Ocean Sampling Networks (AOSN). A remarkable contribution was provided by the second phase of the AOSN (AOSN-II) field program performed in Monterey Bay,

Corresponding author address: Alberto Alvarez, CMRE, Science and Technology Organization, NATO, Viale San Bartolomeo 400, 19126 La Spezia, Italy.
E-mail: alvarez@cmre.nato.int

DOI: 10.1175/JTECH-D-13-00214.1

California, from mid-July to early September 2003 (Leonard et al. 2007; Ramp et al. 2009). The experiment applied a wide variety of networked platforms to adaptively sample upwelling events in the coastal ocean and to use the information gathered to improve predictive skill for quantities of interest to end users (Lermusiaux 2007). Demonstration of cooperative control and adaptive sampling of ocean features using a fleet of gliders was also performed as part of the Adaptive Sampling and Prediction (ASAP) project (Leonard et al. 2010). This field experiment effectively emulated a coordinated glider network. The fieldwork during AOSN-II was continued during 2006 in the framework of ASAP (Ramp et al. 2011) to demonstrate automated control of coordinated fleets of gliders proposed in Zhang et al. (2007) and to test more sophisticated fleet formations. Finally, Hayes et al. (2010) sampled a warm core eddy in the Levantine Sea (eastern Mediterranean) using three underwater gliders coordinated in an equilateral triangular formation.

Cooperative and unaware networks gliders have also been studied in the literature. Alvarez et al. (2007) used a genetic algorithm to find optimal glider trajectories to provide, together with an unevenly distributed network of floats, the minimum mean error obtained from an optimum interpolation scheme. Genetic algorithms were also employed by Heaney et al. (2007) to optimize sampling strategies of a fleet of gliders based on the estimated performance of ocean predictions when glider data are assimilated into ocean models. Alvarez and Martinez (2011), Alvarez and Mourre (2012), and Mourre and Alvarez (2012) used simulated annealing and pattern search as optimization engines. Cooperative and unaware networks of gliders have been experimentally implemented in the framework of a military exercise (Osler et al. 2011).

Whether one of these cooperative implementations, cooperative-unaware or coordinated, results in a more efficient sampling of the ocean variability remains an open question. The answer very likely depends on the observational objective. This paper presents an evaluation of both strategies through numerical experiments in the northern Ligurian Sea (western Mediterranean). The study first extends the method to determine optimum sampling trajectories of cooperative-unaware glider networks developed in Alvarez and Mourre (2012) to the case of coordinated glider networks. The extended approach is then applied to evaluate the capabilities of unaware and coordinated networks of gliders at reducing the temperature uncertainty in numerical model predictions of the northern Ligurian Sea. Consistent with previous studies in this area (Alvarez and Mourre 2012; Mourre and Alvarez 2012), temperature was chosen as the study variable for its predominant impact on density and sound speed fields, and its direct link with mesoscale activity. Observing system simulation experiments (OSSEs; Hackert et al. 1998; Mourre et al. 2006; Ballabrera-Poy et al. 2007) are used in this work to evaluate the performance of cooperative and coordinated sampling strategies with gliders. The article is organized as follows: section 2 describes the design of the OSSE, section 3 presents the results, and section 4 concludes the article.

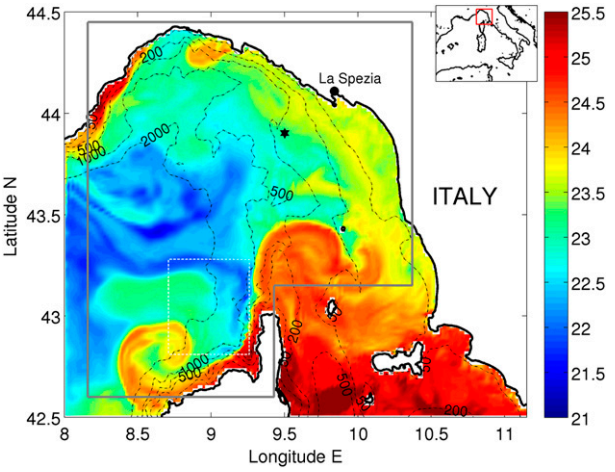

FIG. 1. SST (°C) of the model nature run for 21 Aug. The gray polygon delimits the area considered for the OSSE. The white rectangle defines a local validation subdomain. The starting point for the glider missions is marked by the black star.

2. Design of the OSSE

a. *Numerical modeling and data assimilation*

An OSSE has been implemented in the Ligurian Sea, the northernmost area of the western Mediterranean Sea (Fig. 1). The oceanic circulation in the Ligurian Sea is simulated by means of a regional configuration of the Regional Ocean Modeling System (ROMS; Haidvogel et al. 2008). The modeling domain covers the entire Ligurian Sea, with two open boundaries on the western and southern sides (located at 8°E and 42.5°N, respectively). The horizontal resolution of the model grid is around 1.8 km. The vertical grid uses 32 sigma-coordinate levels, which are nonlinearly stretched to allow a finer resolution of the surface boundary layer. The 7-km-resolution atmospheric model Consortium for Small-Scale Modeling–Mediterranean (COSMO-ME) of the Italian Air Force National Meteorological Center [Centro Nazionale di Meteorologia e Climatologia Aeronautica (CNMCA); Bonavita and Torrisi 2005] provides the atmospheric data necessary to compute the surface fluxes of momentum, heat, and freshwater. The large-scale

Mediterranean Forecasting System (MFS) model outputs (Oddo et al. 2009) are used to initialize the model on 1 May 2010 and to calculate the fluxes through the two open boundaries using the algorithm proposed by Marchesiello et al. (2001). The external forcing also includes climatological runoffs from the rivers Arno, Magra, and Serchio. The model was run in forecast mode without assimilation from 1 May to 21 August 2010. A more detailed description of the model configuration can be found in Alvarez et al. (2013). An asynchronous formulation of the ensemble Kalman filter (EnKF) approach (Evensen 2003; Sakov et al. 2010) is used to assimilate temperature observations in the model. The asynchronous formulation, which allows the assimilation of observations taken at a time different from the time of the analysis, uses a 48-h window to cover the entire glider mission cycle. At a given time, the method produces an analysis ensemble of model states based on the statistical impact of all the observations collected during the previous 48 h. Notice the difference with other filters where the effect of these observations might be additionally integrated by the model equations from the observation to the update time. The full set of equations describing the present implementation of the ensemble Kalman filter can be found in Mourre and Chiggiato (2014).

Perturbations of the initial conditions, winds, and lateral boundary conditions are considered in this study. The reader is referred to Mourre and Chiggiato (2014) for details of the perturbation strategy. A 96-member ensemble is initialized at 0000 UTC 13 August using model states randomly selected among the ROMS reference solutions at 0000 UTC 8–18 August.

Several simulations are typically generated to conduct OSSEs: (i) a nature run that is supposed to represent the ocean truth; (ii) a control run that is perturbed with respect to the nature run, and that represents the solution without assimilation; and (iii) an assimilated run in which simulated observations from the nature run have been assimilated. This study uses a so-called fraternal twin experiment approach, the nature run being provided by the ROMS model forecast simulation that was run operationally during the Recognized Environmental Picture 2010 (REP10) experiment, and that which slightly differs from the above-described ROMS configuration (hindcast version) in terms of model internal and boundary parameters. The control run is the mean of an ensemble of simulations with the same perturbations as those represented in the EnKF (i.e., of the initial conditions, winds, and lateral boundary values). The reduction of the error (defined as the difference with the nature run) from the control run to the assimilated run provides a measure of the performance of the assimilation procedure.

b. *Optimum mission planning of glider networks*

Ideally, to determine the configuration of the observing network with the best performance for the next 48 h, an EnKF analysis should be performed for each tentative network configuration after having simulated the 48-h ensemble forecast (Majumdar et al. 2002; Lermusiaux 2007). In this work, to limit the computational cost and to allow a larger number of iterations, this procedure was simplified by considering the vertical and time-averaged fields over the glider diving depth and over the 48-h forecast period. Projecting the original field information onto a two-dimensional field by using the average or integral uncertainty values over depth was previously used in the context of adaptive sampling (Yilmaz 2006; Yilmaz et al. 2008). This assumes that a network configuration that minimizes the uncertainty of the depth- and time-averaged fields will also minimize (or closely minimize) the uncertainty of the whole four-dimensional fields. This can be justified by the shortness of the vertical correlation lengths and forecast period. Given a glider network configuration and the error covariance matrix of the two-dimensional field representing the surface to 100 m and 48-h averaged temperature, the variance-minimizing analysis provides an estimate of the corresponding posteriori error covariance matrix, which measures the reliability of field estimations when observations are available at certain locations. Glider trajectories can be planned in such a way that the estimations of the field at the grid points optimize a certain norm of the posteriori error covariance matrix. Alvarez and Mourre (2012) found that minimizing the norm defined by the trace of the posterior covariance with respect to the observation locations was the most adequate strategy to sample the environment.

The method detailed in Alvarez and Mourre (2012) is applied to generate tentative trajectories for cooperative and unaware networks during the trace minimization process. For coordinated configurations, the approach needs slight modifications. Specifically, a regular pattern describing the fixed location of the gliders relative to the barycenter (BC; point at the center) of the fleet is first defined. The trajectory of the jth glider in the fleet is reconstructed from a sequence of waypoints of the barycenter, $\Gamma_{\mathrm{BC}} = \{\mathbf{x}_o^{\mathrm{BC}}, \mathbf{x}_1^{\mathrm{BC}}, \ldots, \mathbf{x}_M^{\mathrm{BC}}\}$, which is also obtained from the algorithm described in Alvarez and Mourre (2012). The headings at the ith waypoint of the barycenter, $\mathbf{x}_i^{\mathrm{BC}}$, determine the orientation of the coordinated pattern in the segment $\{\mathbf{x}_i^{\mathrm{BC}}, \mathbf{x}_{i+1}^{\mathrm{BC}}\}$. Control procedures to maintain the fleet formation are not simulated in this work. This implicitly assumes that the depth-averaged current field is not strong enough to induce significant deviations from the glider navigation

determined from dead reckoning. This assumption has been experimentally confirmed in the case of deep gliders operating in the marine area under consideration (the average deviation from waypoints for a deep glider diving down to 500-m depth was 1.3 ± 1 km during a recent field trial conducted in this area). In both cooperative-unaware and coordinated cases, sampling missions are considered feasible if all glider trajectories are confined in the area of operations. Finally, glider observations are located every kilometer along the simulated glider trajectories in both network configurations. This would correspond to the horizontal sampling resolution of a deep Slocum glider diving down to 500-m depth.

Similar to Alvarez and Mourre (2012), a pattern search optimization (PSO) approach (Hooke and Jeeves 1961; Coope and Price 2002) is used in this study to minimize the trace of the a posteriori covariance with respect to the glider trajectories.

3. Results

The OSSE described in the previous section starts at 0000 UTC 21 August. A forecast of the physical evolution and associated uncertainty in the selected marine region is generated for the 48-h period ranging from 21 to 23 August. The expected uncertainty derived from the ensemble run is used to determine cooperative-unaware and coordinated sampling strategies for a fleet of three gliders. All gliders in the cooperative-unaware formation were initially located at 43°54′N and 9°30′E offshore La Spezia, Italy (see Fig. 1). In the coordinated case, this initial location defined the barycenter of an equilateral triangle with 25-km edges, on the nodes of which the gliders were positioned. This is the minimum edge length required to embed into the triangle formation dynamical structures with horizontal scales equal to the Rossby radius of deformation, which is on the order of 12 km in this region (Grilli and Pinardi 1998).

Figures 2a,b display the temperature fields averaged in the vertical over the glider diving depth and in time over the 48-h period ranging from 21 to 23 August for the nature and control runs, respectively. The main differences between the nature and control solutions are a warm eddy structure located along the northwestern Corsica coast present in the nature run and slightly colder waters along the Ligurian coast in the control run.

a. Cooperative-unaware network

Figures 3 summarizes the results obtained for the different assimilation cycles of the cooperative-unaware network. Optimum glider trajectories and the expected uncertainty in the temperature field averaged in the vertical over the glider diving layer and in time over the 48-h forecast period are shown in Figs. 3a–d. Two gliders are initially directed to the central and southern regions of the basin, where significant uncertainty is generated by the convergence of two major current systems (the Tyrrhenian Current outflowing from the Tyrrhenian Sea and the West Corsica Current) and by the propagation along the Corsican coast of eddies of different sizes and positions in the different realizations of the ensemble. Notice that even if the control solution, which is the ensemble mean solution, does not properly represent the eddy (Fig. 2b) because of its variability across the ensemble members, the associated uncertainty is properly captured in the ensemble. The third glider moves northward to prevent sampling redundancy with the other two platforms. The data collected during the first 2 days have allowed for reduction of a large part of the

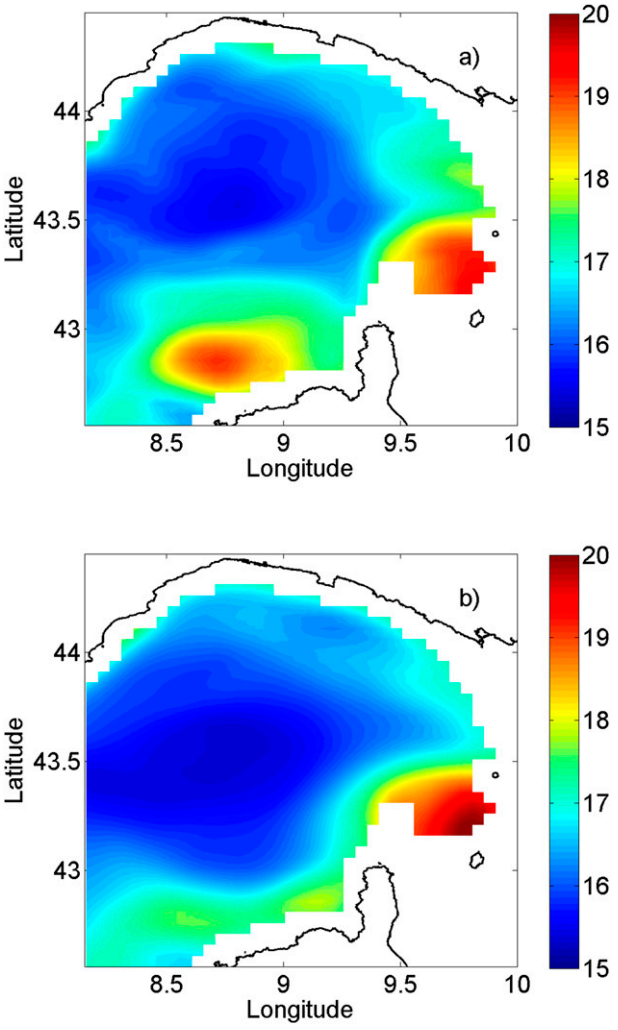

FIG. 2. Temperature field (°C) for the period 21–23 Aug for the (a) nature run and (b) control run.

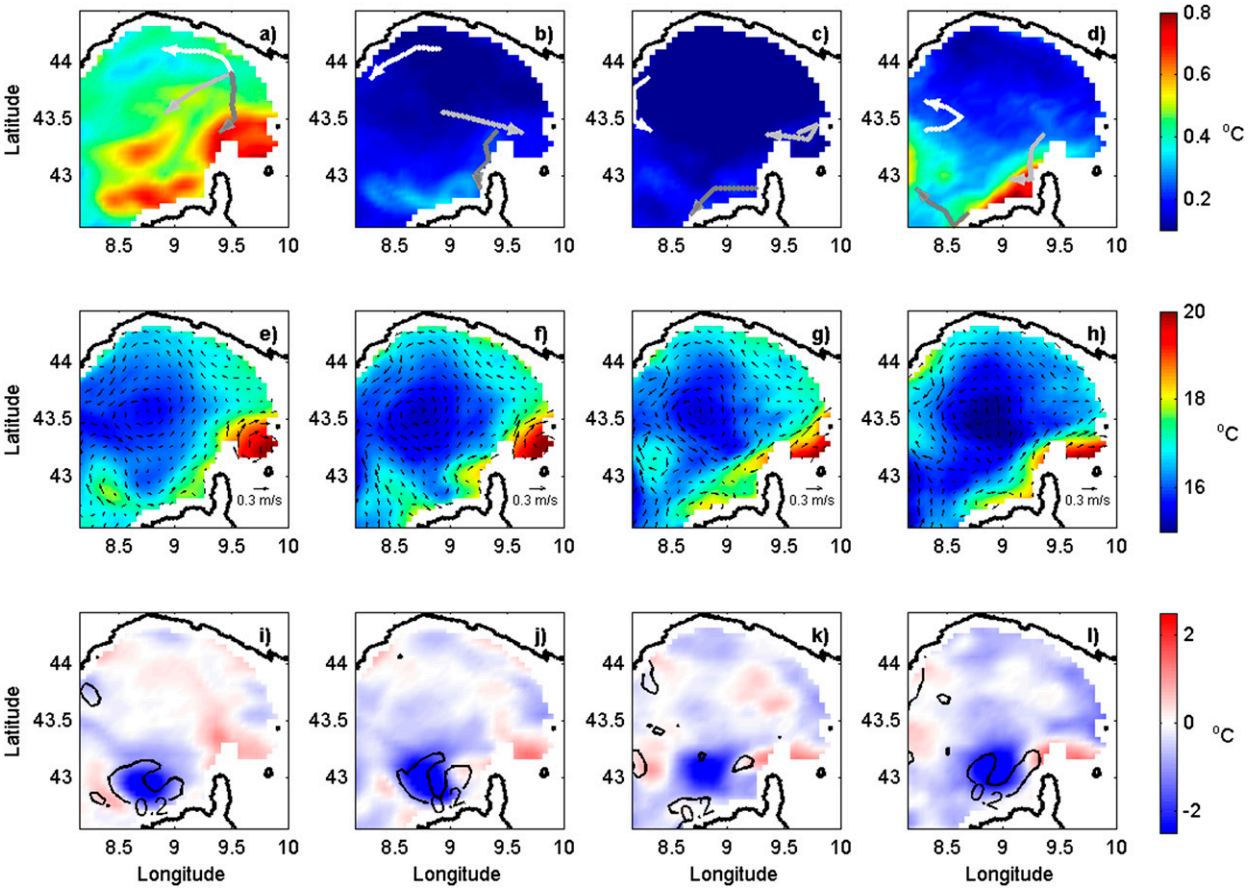

FIG. 3. Forecast error (°C) of the average temperature and optimum glider tracks (lines) for the period (a) 21–23 Aug, (b) 23–25 Aug, (c) 25–27 Aug, and (d) 27–29 Aug from the cooperative-unaware scenario. Average temperature and currents for the forecast periods (e) 23–25 Aug, (f) 25–27 Aug, (g) 27–29 Aug, and (h) 29 Aug–1 Sep. The color field displays differences of the predicted temperature with the nature run for the forecast period (i) 23–25 Aug, (j) 25–27 Aug, (k) 27–29 Aug, and (l) 29 Aug–1 Sep. The 0.2 m s^{-1} contour of the modulus of the velocity error is also shown in (i)–(l). This is the maximum modulus of the velocity error with certain spatial coherence.

initial uncertainty (Fig. 3b). This significant reduction of the ensemble spread over the whole domain mainly reflects the reduction of the model error associated with the initial condition perturbations, which tend to generate large-distance covariance. The mean uncertainty then remains relatively low during the next two cycles because of a calm weather period. However, the residual uncertainty in the area of the missing eddy is still able to drive one of the platforms toward this area, leading to a sampling of the southern part of the eddy by one of the gliders during the third assimilation cycle (Fig. 3c). The temperature fields averaged in the vertical over the glider diving layer and in time over the 48-h forecast period (Figs. 3e–h) do not reveal any significant improvement of the prediction performance due to the inability to properly represent the eddy structure with the available sampling by a single glider. Thus, significant errors persist in that area in both temperature and velocity fields.

b. *Coordinated network*

The case of the coordinated network of gliders is summarized in Fig. 4. The fleet is directed southward to sample the region with the largest uncertainty (Fig. 4a) during the first assimilation cycle, and then it follows a westward zigzag motion along the northwestern coast of Corsica (Figs. 4b–d). The glider fleet moves as a whole between the waypoints, which are computed for the barycenter for all assimilation cycles. Based on a leader–follow strategy, the triangle formation rotates when a waypoint is reached to head the leader glider toward the next waypoint. Notice that no observations from the fleet are assumed when rotating around the barycenter, inducing apparent discontinuity between tracks. This assumption is justified by the relatively small motions resulting from the heading of the fleet when compared to the total tracks. It also permits keeping the same number of observations for different sizes of the triangle formation.

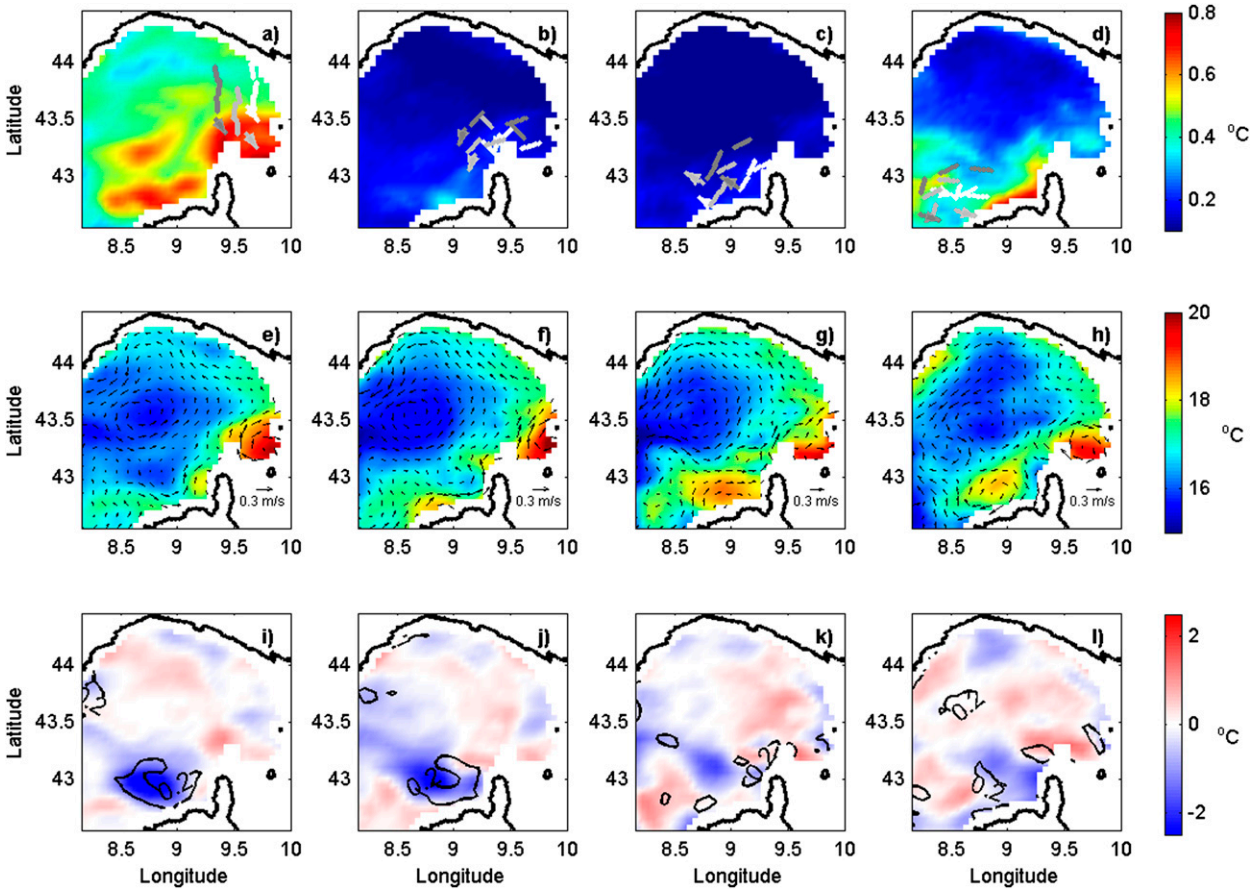

FIG. 4. As in Fig. 3, but for the coordinated network.

The temperature fields and associated currents averaged in the vertical over the glider diving layer and in time over the 48-h forecast period are plotted in Figs. 4e–h. In contrast to the cooperative-unaware network, a warm core eddy is inserted and maintained north of Corsica during the third and fourth assimilation cycles (Figs. 4g,h). The evolution of the error field (Figs. 4i–l) shows a significant reduction of the missing warm eddy signal in the last two forecast cycles.

c. *Intercomparison of the performance of the cooperative-unaware and coordinated glider networks*

The OSSE domain has been divided into two subdomains to further quantify the performance of the cooperative-unaware and coordinated networks. The first subdomain is defined by a rectangular polygon embedding the eddy located offshore of the northwestern

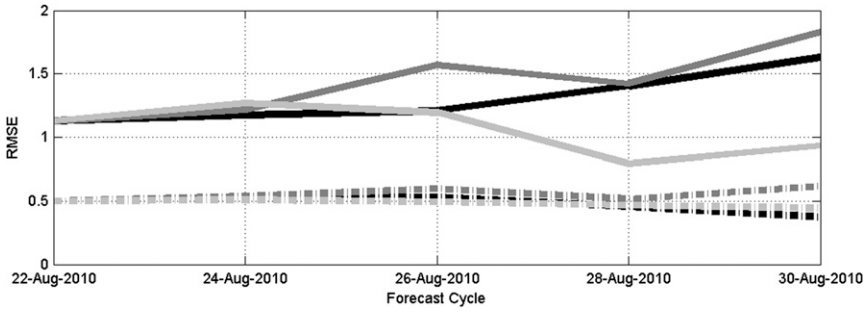

FIG. 5. RMSE for the different forecast cycles for the control run (black lines), assimilated run from the cooperative-unaware network (dark gray lines), and assimilated run from the coordinated network (light gray lines) in the eddy (solid lines) and basin (dotted lines) subdomains.

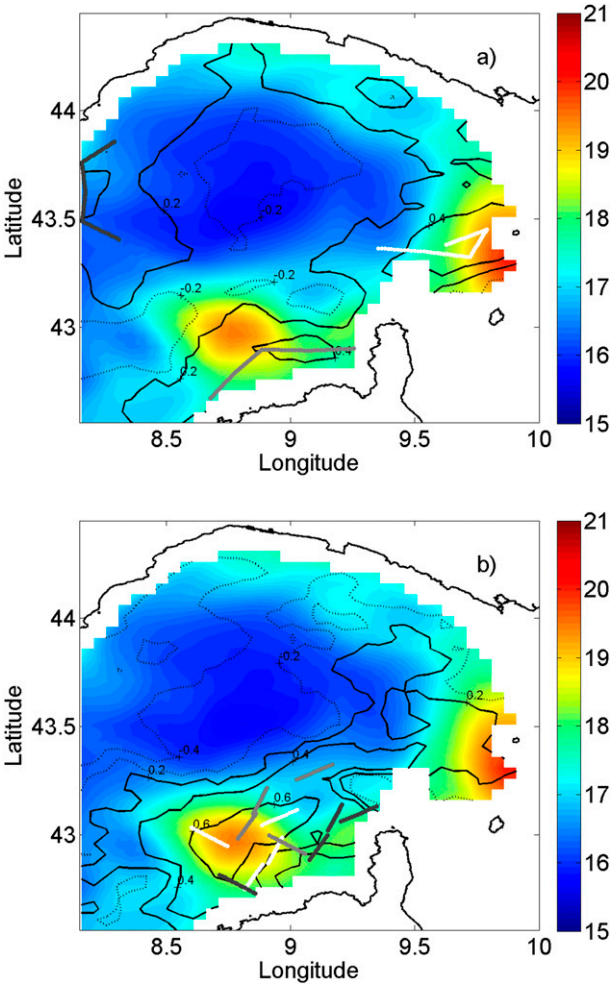

FIG. 6. (a) Glider trajectories for the cooperative-unaware network during the assimilation period 23–25 Aug. The color field represents the depth- and time-averaged temperature field of the nature run. Contours show the correlation coefficient averaged over the observations derived from the ensemble covariance for this period. (b) As in (a), but for the coordinated network.

Corsican coast (see Fig. 1). The remaining area constitutes the second subdomain. Figure 5 displays the root-mean-square error (RMSE) obtained from the different cases in both subdomains for the successive forecast cycles. The figure indicates a significant improvement of the forecast performance at the eddy location obtained from the coordinated glider fleet during the forecast cycle centered on 28 August (third cycle). Conversely, the forecasts resulting from the cooperative-unaware network in this subdomain slightly degrade the performance compared to the solution without any data assimilation. Forecast performances are comparable for all cases in the remaining subdomain with a lower mean error, indicating a negligible impact of the observations on the model results.

Figures 6a,b clarify the dissimilarity found between the forecast performances of the coordinated and the cooperative-unaware networks after the third assimilation cycle. The figures display (for each sampling scenario) the nature run temperature field, the particular observations collected during this cycle, and the isolines of correlation coefficients derived from the corresponding ensemble covariance and averaged over the particular observations. Figure 6a shows that the glider from the cooperative-unaware network does not sample the core of the eddy. Moreover, this core lies in an area poorly correlated with glider observations. Instead, the core of the eddy is monitored by two of the gliders in the coordinated network, resulting in a substantially higher impact of the observations over the eddy location (Fig. 6b). As a result, the eddy is inserted during the forecast cycle from 27 to 29 August and maintained during the forecast cycle from 29 August to 1 September in the case of the coordinated network (Figs. 4g,h), contrary to the cooperative network (Figs. 3g,h).

d. Intercomparison of the performance of coordinated glider networks with triangular formation and different edge size

Additional OSSEs have been performed to investigate the dependence of the performance of the coordinated glider network on the edge size of the triangular formation. Specifically, glider fleets coordinated in equilateral triangles of 10- and 40-km edges have been further considered. The resulting optimum sampling trajectories for both cases (not shown) resemble those obtained with the case of a triangular formation with a 25-km edge. Figure 7 displays the RMSE obtained for the different subdomains and coordinated network configurations. All network configurations reduce the RMSE in the subdomain, embedding the eddy during the forecast cycle centered on 28 August, when the platforms enter this particular area. The best performance is achieved by the network with a 10-km edge because of its higher spatial resolution. The error then increases for this network during the last cycle because observations partially cover the eddy (Fig. 8a). The coarser-resolution sampling configuration leads to a further reduction of the error during the last cycle because of the larger spatial coverage of the eddy, after the rotation of the fleet formation constrained by model boundaries (Fig. 8b). Regarding the second subdomain, the best performance is obtained by the network configuration with the intermediate resolution. Notice that the sampling of the eddy area with large uncertainty together with the long-distance correlations present in the ensemble leads to corrections of the temperature fields in this subdomain. The degradation of

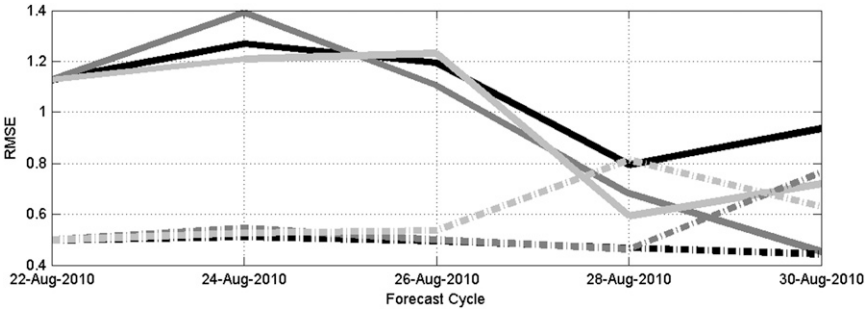

FIG. 7. RMSE for the different forecast cycles with the coordinated network with a 40-km edge (dark gray lines) and a 10-km edge (light gray lines) in the eddy (solid lines) and basin (dotted lines) subdomains. Results from the coordinated triangular network with a 25-km edge (black solid and dotted lines) are also included to facilitate the intercomparison.

the forecast accuracy in two of the three scenarios reveals the need to apply covariance localization during the assimilation process, which was not done in this study.

4. Discussion and conclusions

This article has evaluated the performance of cooperative-unaware and coordinated networking approaches for glider fleets with OSSEs during an 8-day period in the Ligurian Sea. A fleet of three gliders was considered in the simulation studies. This is the minimum number of gliders required to define a geometric formation able to enclose ocean structures like eddies, thus providing snapshots of spatial gradients. The question of the optimum number of platforms and the best geometric patterns to resolve ocean structures was out of the scope of the present study (see L'Hévéder et al. 2013 regarding this issue). Basic dynamical parameters of the region of interest were employed as guidelines to the initial network and mission design. Specifically, the updating mission cycles and the spatial configuration of the coordinated network were fixed to match the expected synoptic time scale and the Rossby radius of deformation in the area, respectively. This approach aimed to resolve the most significant spatial and temporal scales. At this stage, glider trajectories remain the only degree of freedom to further improve the sampling performance of the observing network.

The OSSEs conducted in this study indicate that the coordinated network leads to a better forecast performance when compared to the cooperative-unaware behavior. The improved performance in the coordinated case is closely linked to the existence of a well-defined and localized eddy structure in the domain. They also show that the impact of observations on the forecast performance is much less significant outside the eddy area. The former is explained by the fact that the

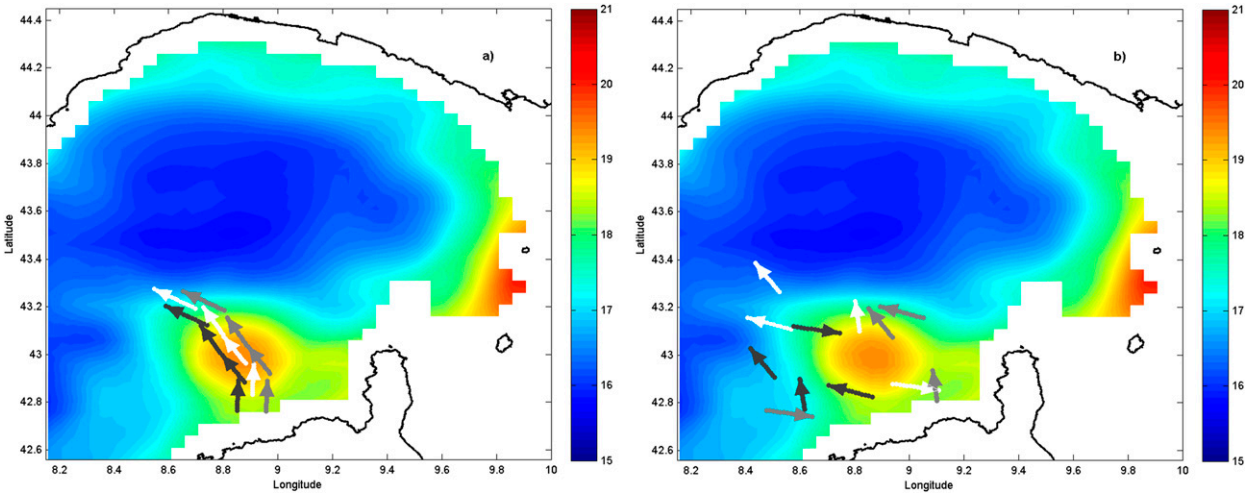

FIG. 8. Optimum glider tracks (lines) from the coordinated scenario with (a) a 10-km edge and (b) a 40-km edge for the period 27–29 Aug. The color field represents the temperature (°C) from the nature run for the period 27–29 Aug.

sampling coverage of the eddy by the coordinated fleet is superior to that provided by the cooperative-unaware network. The latter indicates that the accuracy of the observations is not sufficient to further reduce the low initial uncertainty level in this subdomain.

While the superior performance of the coordinated network is evident from the OSSEs, the dependence of this performance on the size of the network geometry requires a more subtle interpretation. The increase of the forecast performance of the network with the largest geometry in the last assimilation cycle is attributed to the fact that the eddy is still fully covered by the fleet. This issue addresses the question of the adequacy of the cost function to improve forecasts when ocean structures are present in the domain of interest. When no dominant ocean structure is present, the best performance is obtained by the coordinated network geometry that matches the Rossby radius expected in the region.

To conclude, coordinated glider formations are preferred to sample marine areas where eddy structures are likely to be present. Performance metrics based on variance-oriented criterion may not be suitable under this circumstance because they do not originate sampling strategies dense enough to resolve defined structures. No remarkable differences in performance between cooperative-unaware and coordinated formations have been found in regions with no dominant ocean features. Further, no significant improvement due to the assimilation has been identified in these regions of low uncertainty level. Consequently, methodologies are required to assess the number of platforms required to monitor a given region with a prescribed uncertainty threshold.

Acknowledgments. The authors thank Jacopo Chiggiato for running the operational ROMS during the REP10 experiment and for providing the model configuration. This work has been funded by NATO's Allied Command Transformation.

REFERENCES

Alvarez, A., and M. Martinez, 2011: A Matlab package for mission generation of a fleet of gliders. Version 1.0, CMRE Scientific Rep. NURC-SP-2011-003, 20 pp.

——, and B. Mourre, 2012: Optimum sampling designs for a glider–mooring observing network. *J. Atmos. Oceanic Technol.,* **29,** 601–612, doi:10.1175/JTECH-D-11-00105.1.

——, B. Garau, and A. Caiti, 2007: Combining networks of drifting profiling floats and gliders for adaptive sampling of the ocean. *2007 IEEE International Conference on Robotics and Automation,* IEEE, 157–162, doi:10.1109/ROBOT.2007.363780.

——, J. Chiggiato, and B. Mourre, 2013: Under the sea: Rapid characterization of restricted marine environments. *IEEE Rob. Autom. Mag.,* **20,** 42–49, doi:10.1109/MRA.2012.2220505.

Bachmayer, R., N. E. Leonard, J. Graver, E. Fiorelli, P. Battha, and D. Palley, 2004: Underwater gliders: Recent developments and future applications. *UT'04: International Symposium on Underwater Technology, 2004,* IEEE, 195–200, doi:10.1109/UT.2004.1405540.

Ballabrera-Poy, J., E. Hackert, R. Murtugudde, and A. J. Busalacchi, 2007: An observing system simulation experiment for an optimal moored instrument array in the tropical Indian Ocean. *J. Climate,* **20,** 3284–3299, doi:10.1175/JCLI4149.1.

Bonavita, M., and L. Torrisi, 2005: Impact of a variational objective analysis scheme on a regional area numerical model: The Italian Air Force weather service experience. *Meteor. Atmos. Phys.,* **88,** 39–52, doi:10.1007/s00703-003-0071-6.

Coope, I. D., and C. J. Price, 2002: Positive bases in numerical optimization. *Comput. Optim. Appl.,* **21,** 169–175, doi:10.1023/A:1013760716801.

Curtin, T., J. Bellingham, J. Catipovic, and D. Webb, 1993: Autonomous oceanographic sampling networks. *Oceanography,* **6,** 86–94, doi:10.5670/oceanog.1993.03.

Dickey, T.-D., 2003: Emerging ocean observations for interdisciplinary data assimilation systems. *J. Mar. Sys.,* **40–41,** 5–48, doi:10.1016/S0924-7963(03)00011-3.

Eriksen, C. C., T. J. Osse, R. D. Light, T. Wen, T. W. Lehman, P. L. Sabin, J. W. Ballard, and A. M. Chiodi, 2001: Seaglider: A long-range autonomous underwater vehicle for oceanographic research. *IEEE J. Oceanic Eng.,* **26,** 424–436, doi:10.1109/48.972073.

Evensen, G., 2003: The ensemble Kalman filter: Theoretical formulation and practical implementation. *Ocean Dyn.,* **53,** 343–367, doi:10.1007/s10236-003-0036-9.

Farinelli, A., L. Iocchi, and D. Nardi, 2004: Multirobot systems: A classification focused on coordination. *IEEE Trans. Syst. Man Cybern.,* **34B,** 2015–2028, doi:10.1109/TSMCB.2004.832155.

Grilli, F., and N. Pinardi, 1998: The computation of Rossby radii of deformation for the Mediterranean Sea. *MTP News,* Vol. 6, No. 4, GRC Geociènces Marines, Universitat de Barcelona, Barcelona, Spain, 1 p.

Hackert, E. C., R. N. Miller, and A. J. Busalacchi, 1998: An optimized design for a moored instrument array in the tropical Atlantic Ocean. *J. Geophys. Res.,* **103,** 7491–7509, doi:10.1029/97JC03206.

Haidvogel, D. B., and Coauthors, 2008: Ocean forecasting in terrain-following coordinates: Formulation and skill assessment of the Regional Ocean Modeling System. *J. Comput. Phys.,* **227,** 3595–3624, doi:10.1016/j.jcp.2007.06.016.

Hayes, D., and Coauthors, 2010: Glider transects in the Levantine Sea: A study of the warm core Cyprus eddy. Rapport Commission International Mer Méditerranée 39, CIESM, 116. [Available online at http://www.ciesm.org/online/archives/abstracts/pdf/39/PG_0116.pdf.]

Heaney, K. D., G. Gawarkiewicz, T. F. Duda, and P. F. J. Lermusiaux, 2007: Nonlinear optimization of autonomous undersea vehicle sampling strategies for oceanographic data assimilation. *J. Field Robot.,* **24,** 437–448, doi:10.1002/rob.20183.

Hooke, R., and T. A. Jeeves, 1961: ''Direct search'' solution of numerical and statistical problems. *J. Assoc. Comput. Mach.,* **8,** 212–229, doi:10.1145/321062.321069.

Kunzig, R., 1996: A thousand diving robots. *Discover Mag.,* **17,** 60–63.

L'Hévéder, B., L. Mortier, P. Testor, and F. Lekien, 2013: A glider network design study for a synoptic view of the oceanic

mesoscale variability. *J. Atmos. Oceanic Technol.,* **30,** 1472–1493, doi:10.1175/JTECH-D-12-00053.1.

Leonard, N. E., D. Paley, F. Lekien, R. Sepulchre, D. M. Frantantoni, and R. Davis, 2007: Collective motion, sensor networks and ocean sampling. *Proc. IEEE,* **95,** 48–74, doi:10.1109/JPROC.2006.887295.

——, ——, R. Davis, D. Fratantoni, F. Lekien, and F. Zhang, 2010: Coordinated control of an underwater glider fleet in an adaptive ocean sampling field experiment in Monterey Bay. *J. Field Robot.,* **27,** 718–740, doi:10.1002/rob.20366.

Lermusiaux, P. F., 2007: Adaptive modeling, adaptive data assimilation and adaptive sampling. *Physica D,* **230,** 172–196, doi:10.1016/j.physd.2007.02.014.

Majumdar, S. J., C. H. Bishop, B. J. Etherton, and Z. Toth, 2002: Adaptive sampling with the ensemble transform Kalman filter. Part II: Field program implementation. *Mon. Wea. Rev.,* **130,** 1356–1369, doi:10.1175/1520-0493(2002)130<1356:ASWTET>2.0.CO;2.

Marchesiello, P., J. C. McWilliams, and A. Shchepetkin, 2001: Open boundary conditions for long-term integration of regional oceanic models. *Ocean Modell.,* **3,** 1–20, doi:10.1016/S1463-5003(00)00013-5.

Mourre, B., and A. Alvarez, 2012: Benefit assessment of glider adaptive sampling in the Ligurian Sea. *Deep-Sea Res.,* **68,** 68–78, doi:10.1016/j.dsr.2012.05.010.

——, and J. Chiggiato, 2014: A comparison of the performance of the 3D super-ensemble and an ensemble Kalman filter for short-range regional ocean prediction. *Tellus,* **66A,** 21640, doi:10.3402/tellusa.v66.21640.

——, P. De Mey, Y. Menard, F. Lyard, and C. Le Provost, 2006: Relative performance of future altimeter systems and tide gauges in constraining a model of North Sea high-frequency barotropic dynamics. *Ocean Dyn.,* **56,** 473–486, doi:10.1007/s10236-006-0081-2.

Oddo, P., M. Adani, N. Pinardi, C. Fratianni, M. Tonani, and D. Pettenuzzo, 2009: A nested Atlantic-Mediterranean Sea general circulation model for operational forecasting. *Ocean Sci. Discuss.,* **6,** 1093–1127, doi:10.5194/osd-6-1093-2009.

Osler, J., R. Stoner, and D. Cecchi, 2011: Gliders debut at Proud Manta 11 as data-gathering platforms. *Sea Technol.,* **52,** 37–41.

Ramp, S. R., and Coauthors, 2009: Preparing to predict: The Second Autonomous Ocean Sampling Network (AOSN-II) experiment in the Monterey Bay. *Deep-Sea Res. II,* **56,** 68–86, doi:10.1016/j.dsr2.2008.08.013.

——, P. F. Lermusiaux, I. Shulman, Y. Chao, R. E. Wolf, and F. L. Bahr, 2011: Oceanographic and atmospheric conditions on the continental shelf north of the Monterey Bay during August 2006. *Dyn. Atmos. Oceans,* **52,** 192–223, doi:10.1016/j.dynatmoce.2011.04.005.

Rudnick, D. L., R. E. Davies, C. C. Eriksen, D. M. Fratantoni, and M. J. Perry, 2004: Underwater gliders for ocean research. *Mar. Technol. Soc. J.,* **38,** 73–84, doi:10.4031/002533204787522703.

Sakov, P., G. Evensen, and L. Bertino, 2010: Asynchronous data assimilation with the EnKF. *Tellus,* **62A,** 24–29, doi:10.1111/j.1600-0870.2009.00417.x.

Sherman, R. E., R. Davis, W. B. Owens, and J. Valdes, 2001: The autonomous underwater glider "Spray." *IEEE J. Oceanic Eng.,* **26,** 437–446, doi:10.1109/48.972076.

Testor, P., and Coauthors, 2010: Gliders as a component of future observing systems. *Proceedings of OceanObs'09: Sustained Ocean Observations and Information for Society,* J. Hall, D. E. Harrison, and D. Stammer, Eds., Vol. 2, ESA Publ. WPP-306, doi:10.5270/OceanObs09.cwp.89.

Webb, D. C., P. J. Simonetti, and C. P. Jones, 2001: SLOCUM: An underwater glider propelled by environmental energy. *IEEE J. Oceanic Eng.,* **26,** 447–452, doi:10.1109/48.972077.

Yilmaz, N. K., 2006: Path planning of autonomous underwater vehicles for adaptive sampling. Ph.D. thesis, Massachusetts Institute of Technology, 244 pp. [Available online at http://hdl.handle.net/1721.1/35618.]

——, C. Evangelinos, P. F. J. Lermusiaux, and N. Patrikalakis, 2008: Path planning of autonomous underwater vehicles for adaptive sampling using mixed integer linear programming. *IEEE J. Oceanic Eng.,* **33,** 522–537, doi:10.1109/JOE.2008.2002105.

Zhang, F., D. M. Fratantoni, D. A. Paley, J. M. Lund, and N. E. Leonard, 2007: Control of coordinated patterns for ocean sampling. *Int. J. Control,* **80,** 1186–1199, doi:10.1080/00207170701222947.